PROGRESS IN COLOR, COLORANTS AND COATINGS

available online @ www.pccc.icrc.ac.ir

Prog. Color Colorants Coat. 9 (2016), 151-162

Ministry of Science, Research and Technology
Institute for Color Science and Technology

Corrosion Resistance Enhancement of AZ91 Magnesium Alloy Using Ni-P Interlayer and Electrophoretic Deposited 3YSZ Coating

A. Shahriari [1], H. Aghajani [1*] and M. G. Hosseini [2]

[1.] Department of Materials Engineering, Faculty of Mechanical Engineering, University of Tabriz, P. O. Box: 51666-16471, Tabriz, Iran.

[2.] Department of Physical Chemistry, Faculty of Chemistry, University of Tabriz, P. O. Box: 51666-16471, Tabriz, Iran.

ARTICLE INFO

Article history:
Received: 05 Mar 2016
Final Revised: 27 Apr 2016
Accepted: 15 May 2016
Available online: 15 May 2016

Keywords:
Zirconia
Electrophoretic deposition
AZ91
Ni- P
Interlayer

ABSTRACT

The zirconia stabilized by 3mol % Y_2O_3 (3YSZ) was applied onto the surface of the magnesium alloy AZ91D using electrophoretic deposition (EPD) from a non- aqueous solution. A Ni-P interlayer between the substrate and YSZ coating was also prepared by electroless plating. Finally, coatings were heat treated in control atmosphere at 400 °C. The preparation, microstructure and corrosion resistance of the coatings were investigated. Scanning electron microscope (SEM) was used to investigate the morphology of coatings. In addition, compositions of surface were determined by X-ray diffraction (XRD). The corrosion resistance of the coatings was evaluated by electrochemical impedance spectroscopy (EIS) in 3.5% NaCl solution. Also, the stability of coating was investigated by the Rockwell C indentation test (VDI 3198 norm). The results indicate that Ni-P interlayer can improve the quality of zirconia coating on the surface. Also, the Ni-P interlayer and YSZ coating increase the charge-transfer resistance of AZ91D surface in chloride solution. Prog. Color Colorants Coat. 9 (2016), 151-162 © Institute for Color Science and Technology.

Archive of SID

1. Introduction

Magnesium and its alloys are the lightest structural metals which their density are about one-fourth of that of steel and two-thirds of that of aluminum. Therefore, they are attractive in automotive, aerospace, power tools and 3C (computer, communication and consumer products) industries. However, magnesium and its alloys are not corrosion resistance under various aqueous or humid conditions. So, the relatively low corrosion resistance of magnesium alloys limits their applications in industries [1].

The simplest way to protect the surface of Magnesium alloys is coating. The coatings can protect the surface by creating a barrier between the surface of alloy and its environment [2]. There are different processes for coating of magnesium and its alloys which each has their own advantages and disadvantages [2]. Organic and inorganic coatings can be applied onto magnesium alloys. Organic coatings

*Corresponding author: h_aghajani@tabrizu.ac.ir

www.SID.ir

usually have poor adhesion if they are applied without an appropriate pre-treatment [3]. Furthermore, inorganic coatings can also be applied onto the surface of the magnesium alloys to improve their corrosion resistance, however, similar to organic coatings, they have poor adhesion to magnesium substrate [4]. The previous studies show that the zirconia coating onto the magnesium alloys can significantly improve the corrosion resistance of these alloys [5, 6].

The ceramic coatings can be applied by the electrophoretic deposition (EPD) that is a simplest and fastest method for coating of inorganic powders from colloidal suspensions [7]. The EPD process includes two steps. First, the charged particles which are suspended in liquid migrate toward an electrode under the effect of electrical field and in the second step, the particles that deposit on the surface of electrode produce a dense, compact and usually thick film [8, 9].

Two groups of parameters affect the characteristics of EPD process: those which are related to the suspension and those related to the physical parameters such as potential, deposition time, the nature of electrodes, etc. During deposition of charged particles onto a substrate by EPD, part of electric current carried not only by the charged particles but also by free ions co-existing in the suspension. In addition, it is believed that the accumulation of ions at the electrodes during the electrophoretic deposition can decrease the deposition rate. On the other hand, the conductivity of the suspension in EPD process is a key factor. Thus, it has been pointed out that if the conductivity of suspension is high, the particle motion will be slow. Therefore, the solubility of the substrate in the suspension can affect the stability and deposition rate of the particles [10]. Also, a heat treatment or high temperature sintering is usually required in order to further densify the deposits and reduce their porosity [9].

The high temperature sintering is a main disadvantage in EPD of ceramic coatings on metal substrate, because the high temperature can damage metal substrate [11]. Another problem is the difference between the expansion coefficients of magnesium alloys and ceramic coatings (about 15×10^{-6} K^{-1} at 20 °C) [12, 13]. Therefore, during thermal treatment, the change of volume of metal substrate can produce stresses which can lead to cracking or even delamination of coating [13].

Some studies show that some metal powders such as Al, Ni can be added to the EPD suspension to increase the density of the ceramic coatings at lower sintering temperatures [11, 14]. Also, the Ni electroless interlayer can improve the adherence and density of the YSZ coating on metal substrate. During the heat treatment, the volume expansion associated with oxidation of Ni can partially increase the density of coating [14]. Electroless plated Ni-P layer has a thermal expansion coefficient of 12×10^{-6} K^{-1} ~ 14×10^{-6} K^{-1} which is close to the thermal expansion coefficient value of magnesium alloy substrate [12].

In other words, Ni–P electroless coating can be a suitable candidate as interlayer between top coat (3YSZ) and magnesium alloy substrate. The Electroless Nickel (EN) plating is a widely used surface modification technology due to superior hardness and corrosion resistance of the deposit [15]. The EN coatings on the magnesium alloys exhibit a nodular morphology with good adherence to substrate [16].

The aim of this study is to apply the YSZ coating on AZ91D alloy by EPD process and investigate the effect of Ni-P interlayer on the compactness of the YSZ coating on AZ91D substrate. Finally, the corrosion resistance of coated alloy was studied.

2. Experimental method

The composition of AZ91D magnesium alloy which was used as the substrate is listed in Table 1. Samples of AZ91D were cut into the size of 12 mm × 12 mm × 2 mm. Before conducting the coating process, the specimens were progressively abraded using emery papers of grade number 80 to 800, then degreased in acetone. Finally, alkaline cleaning was carried out to remove soils and greases.

Table 1: Chemical composition of AZ91D used in this study.

Mg	Al	Zn	Mn	Cu	Ni	Fe
Bal.	8.3	0.35	0.12	0.03	0.002	0.005

Archive of SID

www.SID.ir

In the next step, the electroless plating of Ni-P interlayer was finished by alkaline cleaning, acid pickling, activation, and electroless plating. The solution composition and operation conditions of electroless plating of Ni-P interlayer is listed in Table 2. Also, the samples were heat treated at 400±10 ºC for 60 min in atmosphere-controlled furnace.

Finally, to produce a dense and homogeneous green film of 3YSZ particles on the magnesium alloy with the Ni-P interlayer, the 3YSZ powders (10 g/L) with mean particle size of 50 nm were dispersed in ethanol-acetyl acetone solution with 1:1 volume ratio and then were stirred. Also, I_2 (0.1 g/L) was added to the suspension as an additive for charging the particles in the suspension and the slurry was ultrasonically vibrated for 10 min. Again, the magnesium alloy with the Ni-P interlayer was selected as the cathode and the stainless steel 316L as the anode in the cell of EPD. The distance of the electrodes was fixed at 1 cm during deposition. An applied voltage of 40 V was used for the deposition of 3YSZ particles in a period of 3 min. The coated samples were heat treated at 400±10 ºC in air for 60 min. The test solutions were prepared using analytical grade chemicals (Merck Co.). In addition, the samples were coded based on preparation and coating method that is identified in Table 3.

The surface morphology of the coatings was observed by SEM (Tescan MIRA3 FEG-SEM, Czech Republic). The phase analysis of the samples was determined by X-ray diffraction (EQuniox 3000, France). Furthermore, potentiostatic impedance tests were done in 3.5 wt% NaCl solution at open circuit potential using a potentiostat/galvanostat (EG&G, PARSTAT 2263, USA) equipped with electrochemical impedance spectroscopy (EIS) module.

A 3-electrode setup was used for the EIS tests. In this setup, AZ and YNi-AZ samples were used as the working electrode. The auxiliary electrode and the reference electrode in the cell were 316L stainless steel and saturated calomel electrode (SCE), respectively. To perform these tests, a sinusoidal potential wave with 10 mV amplitude in the frequency range between 100 KHz and 0.01 Hz was applied to the samples.

The coating adhesion to AZ91D substrate was evaluated using Rockwell C indentation which is standard technique commonly used to quantify the interfacial strength of coating-substrate systems. During the Rockwell C indentation test, a cone-shaped diamond 120° tip (200 μm in radius) was indented perpendicularly onto the coating applying a normal 150N. The results of the test were qualitatively evaluated by comparing the SEM images of the crack network [17]. Therefore, the feature with only a few minor cracks after indentation indicates a good bonding while the other features with extensive delamination of the coating indicate very poor adhesion to substrate.

Table 2: Electroless plating procedure of Ni–P on the Mg alloy substrate.

Procedure	Bath Compositions (Per liter)	Condition
Acid pickling	CrO_3=125 g HNO_3(70%)=110 mL	Room temperature, stirring for 60 s
Activation	HF(40%)=358 mL	Room temperature, stiring for 10 min
Ni plating	$NiSO_4 \cdot 6H_2O$=20 HF (40%)=12 ml $C_6H_8O_7 \cdot H_2O$=5 g NH_4F=10 g $NaH_2PO_2 \cdot H_2O$=20g $NH_3 \cdot H_2O$ (25%)=30 ml Thiourea=1×10^{-3}g	75 °C, pH=6.2 stirring for 2 h

www.SID.ir

Table 3: Code of samples based on preparation and coating process.

Code of sample	Preparation method	Coating process
AZ	Uncoated	Uncoated
YNi-AZ	YSZ coating with Ni-P interlay on surface of AZ91 alloy	Electrophoretic deposition of YSZ coating + electroless plating of Ni-P interlayer

3. Results and discussion

3.1. Ni-P interlayer

Ni-P layer was deposited on AZ91D alloy from a bath with pH=6.2 and then was heat treated in the furnace at 400°C. The Ni–P layer is composed of fine nodules that have "cauliflower" shape (Figure 1 (a)). Micro-pores are distributed on the surface of these nodules (Figure 1(b)). Analyzed EDS (Figure 1(c)) of the nodules showed that the compositions of the layer were identified as 0.79 wt.% phosphorus and 75.14 wt.% nickel.

The percentage of P in Ni-P interlayer is related to pH of the bath, so that by increasing the pH, the nickel reduction reaction is accelerated according to equation (1), on the contrary, the phosphorous reduction is retarded according to equation (2). Therefore, in the acidic baths, the percentage of P is more than in basic ones [18].

$$Ni^{2+} + H_2PO_2^- + H_2O \rightarrow Ni + HPO_3^{2-} + 3H^+ \quad (1)$$

$$H_2PO_2^- + \frac{1}{2}H_2 \rightarrow H_2O + OH^- + P \quad (2)$$

1.7 % of magnesium is also detected in the coating that is due to the dissolution of magnesium surface during the fluoride activation and further co-deposition with the Ni during the electroless plating.

Also, as it is seen from Figure 1, some pores are observed between the nodules. They can be related to the H_2 releasing that accompanies with the deposition of Ni-P according to equation (3). Therefore, H_2 produces some micro-pores on the Ni-P surface.

$$2H^+ + 2e^- \rightarrow H_2 \quad (3)$$

The cross section of the Ni-P coating is shown in Figure 2. According to Figure 2, the thickness of the coating is about 32 µm. The coating thickness is usually a function of deposition rate which in turn depends on the bath and plating conditions [19] and complex agents [20]. In other words, the high thickness of Ni-P layer can be related to the time of deposition that is 120 min. On the other hand, by increasing the time of deposition, the probability of formation of pores and porosity increases, however, the Ni-P layer can bond well to substrate because of the existence of a stronger metal-to-metal bonding during the EN deposition [18].

3.2. 3YSZ coating

In order to coat the YSZ particles on AZ91D alloy coated with Ni-P interlayer, the YSZ particles were dispersed in the ethanol-acetyl acetone solution. The YSZ particles charged via adsorption of protons which are formed by the reaction between acetyl acetone/ethanol and iodine. The addition of iodine to ketone solvents can lead to the production of proton and iodide ions as represented by equations (4) and (5) [21]:

$$CH_3 - CO - CH_2 - CO - CH_3 + 2I_2 \rightarrow ICH_2CO - CH_2 - CO - CH_2I + 2I^- + 2H^+ \quad (4)$$

$$CH_3 - CH_2 - OH + I_2 \rightarrow ICH_2 - CH_2 - OH + H^+ + I^- \quad (5)$$

Therefore, the protons generated will be adsorbed on the suspended YSZ particles, making them positively charged. Application of a dc field forces the positively charged YSZ particles to move towards and deposit on the substrate which is cathode.

Archive of SID

www.SID.ir

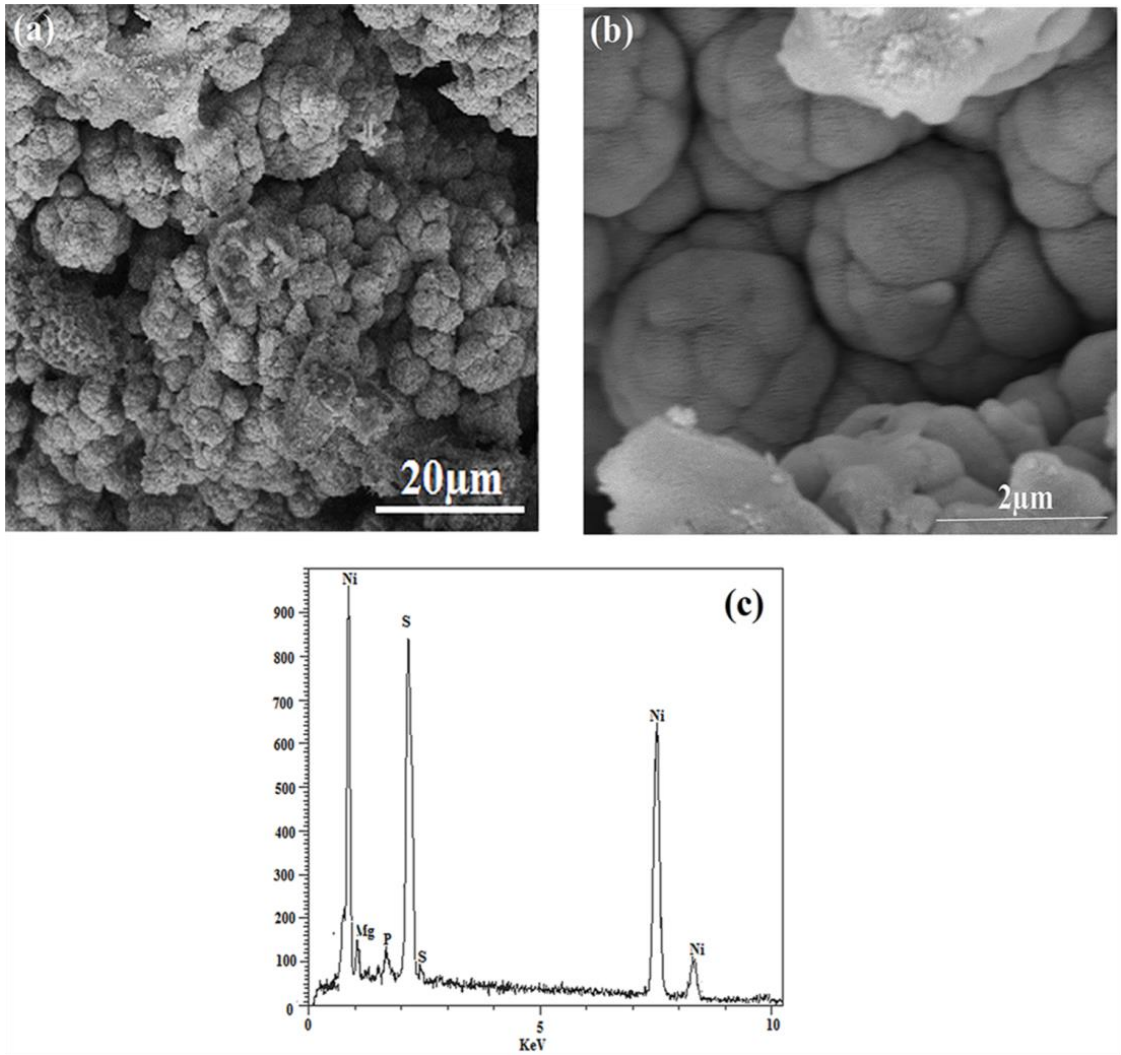

Figure 1: SEM images showing the surface morphologies of the Ni–P layer: (a) low magnification; (b) high magnification (c) the results of the EDS analysis of Ni-P coating on AZ91D alloy.

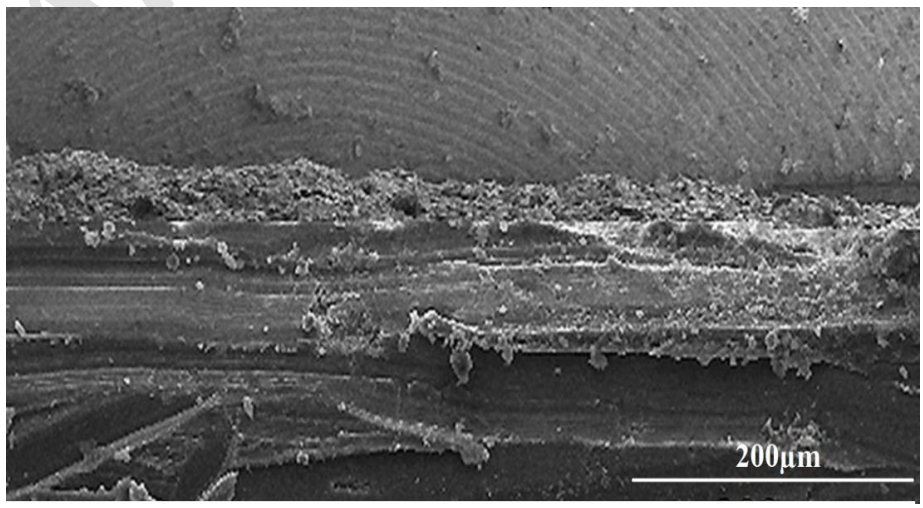

Figure 2: SEM micrographs from cross sections of Ni-P layer on AZ91D alloy.

www.SID.ir

After drying of YSZ coating on the surface of AZ91D alloy with Ni-P interlayer in air, the coating was heat treated at 400 ºC for 60 min. The morphology of YSZ coating on the surface of the magnesium alloy with Ni-P interlayer and without Ni-P interlayer after heat treatment is shown in Figure 3. It should be noted that the numerous cracks are formed in the YSZ coating because of the shrinkage of the coating and loss of water during the heat treatment (Figure 3(a) and (c)). It appears that the agglomerated particles are distributed on both surfaces. Also Figure 3 (b) and (d) show that particle size of the YSZ coating deposited on the magnesium alloy is larger than the particle size of the YSZ on the magnesium alloy with the Ni-P layer. The agglomerated particles are also observable in Figure 3(b). In addition, the statistical analysis carried out by the imager analyzer software (Clemex software) shows that the mean size of YSZ particles on magnesium alloy without Ni-P layer is larger than the mean size of YSZ particles on magnesium alloy with Ni-P layer. Figure 4 shows the cumulative diagram of the particle size of the YSZ coating on magnesium alloy with and without Ni-P layer. The results of the statistical analyses of particle sizes of YSZ coatings are tabulated in Table 4.

Also, it seems that the YSZ particles that are small readily fill the pores between the nodules of Ni-P layer and produce a composite coating including Ni-P-YSZ particles. The YSZ particles which fill the holes can close the ways of transfer of the aggressive species to magnesium alloy surface. The magnesium ions can increase the ionic intensity of the suspension that according to findings of previous studies [22] might have a negative influence on double layer and hence result in reduction of zeta potential of YSZ particles and their lower stability in the solution. Therefore, the presence of Ni-P layer can help to decrease the corrosion of the magnesium alloy. Finally it can improve the quality of the YSZ coating on the magnesium alloy.

On the other hand, the Ni-P interlayer can partially dissolve in acetyl-acetone solution and the Ni^{+2} ions can introduce to solution and form the hydroxide and alkoxide of Ni according to equations (6) and (7):

$$Ni^{2+} + 2OH^{-} \rightarrow Ni(OH)_2 \quad (6)$$

$$2CH_3 - CH_2 - O^{-} + Ni^{2+} \rightarrow Ni(CH_3 - CH_2 - O)_2 \quad (7)$$

The presence of hydroxide can increase the adhesion of YSZ coating to the substrate because the sub-micron particles of hydroxide between the larger particles may enhance the effect of the van der Waals forces and result in an adherent deposit. Also, it is known that the flow of fine powders is hindered by the large attractive forces between the particles. Alternatively the effect of the hydroxide of Ni may be related to its polymeric structure. The flocculation of colloids can be achieved by addition of natural or synthetic polymers of high molecular weight; the polymer chain is assumed to adsorb on to the particles and the bridges are formed of them. Thus a random three-dimensional structure is built which is held together by polymer bridges [23]. Also, nickel hydroxide and nickel alkoxide that are formed can be adsorbed on the surface of YSZ particles to generate charge density and improve the zeta potential of these particles in the suspension.

The XRD pattern from YSZ coating on magnesium alloy without and with Ni-P layer after heat treatment at 400 °C for 60 min is shown in Figure 5. As it is seen from Figure 5(b), the NiP_2 phase is observed, which can help to increase the corrosion resistance of coating. In addition, according to Figure 5(b), The XRD pattern confirms the presence of YSZ phase with the NiO and $NiAl_2O_4$ phases. During the EPD process, the $Ni(OH)_2$ can be formed. Then, the NiO phase would be formed by decomposition of $Ni(OH)_2$ according to Equation (8). Also, it is known that the oxidation of the nickel can take place below 1000 ºC; therefore, it can also be assumed that the NiO can be formed by reaction of the Ni with oxygen in the atmosphere. This reaction is associated with volume expansion that can help to increase the density of the YSZ /Ni-P coating.

$$Ni(OH)_2 \rightarrow NiO + H_2O \quad (8)$$

Archive of SID

www.SID.ir

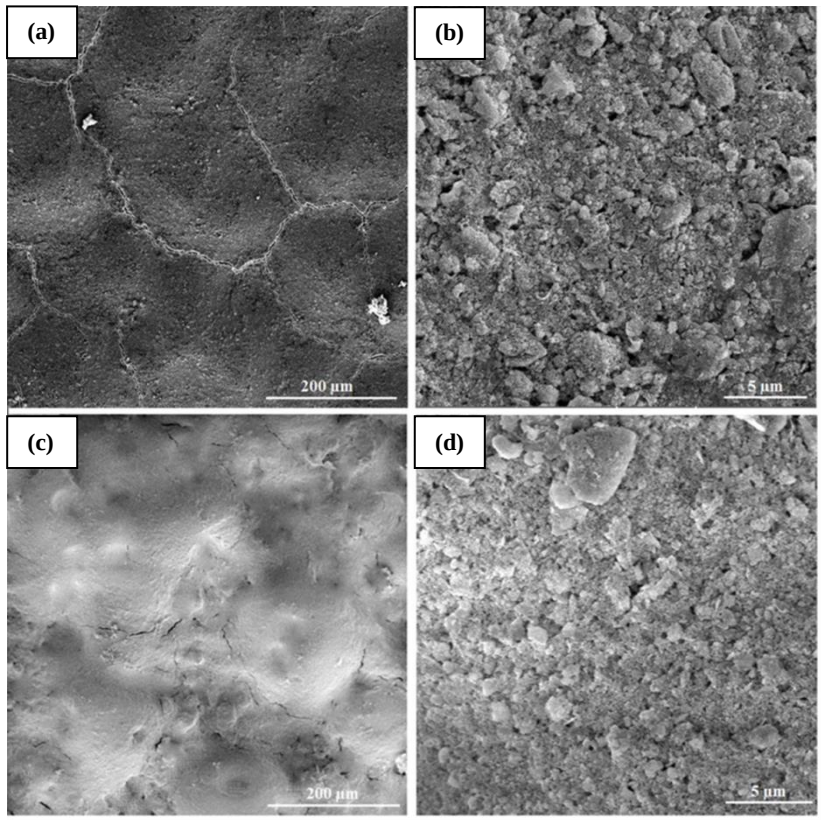

Figure 3: Surface morphology of YSZ coating on AZ91D alloy, (a) and (b) without Ni-P interlayer by low and high magnification, respectively, (c) and (d) AZ91D alloy with Ni-P interlayer by low and high magnification, respectively.

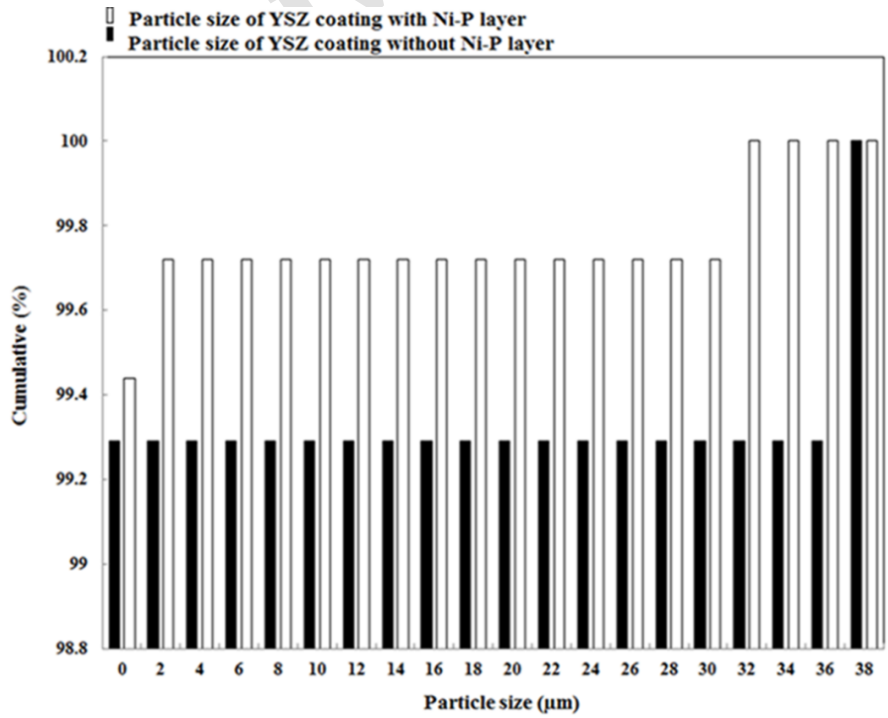

Figure 4: cumulative particle size of YSZ coatings on magnesium alloy with and without Ni-P layer.

www.SID.ir

Table 4: results of particles size of YSZ coating with Ni-P and without Ni-P layer.

Particle Size	Minimum (nm)	Maximum(µm)	Mean(µm)	Standard deviation(µm)
YSZ coating with Ni-P layer	50.5	33.9	0.304	2.14
YSZ coating without Ni-P layer	50.5	38.2	0.373	3.22

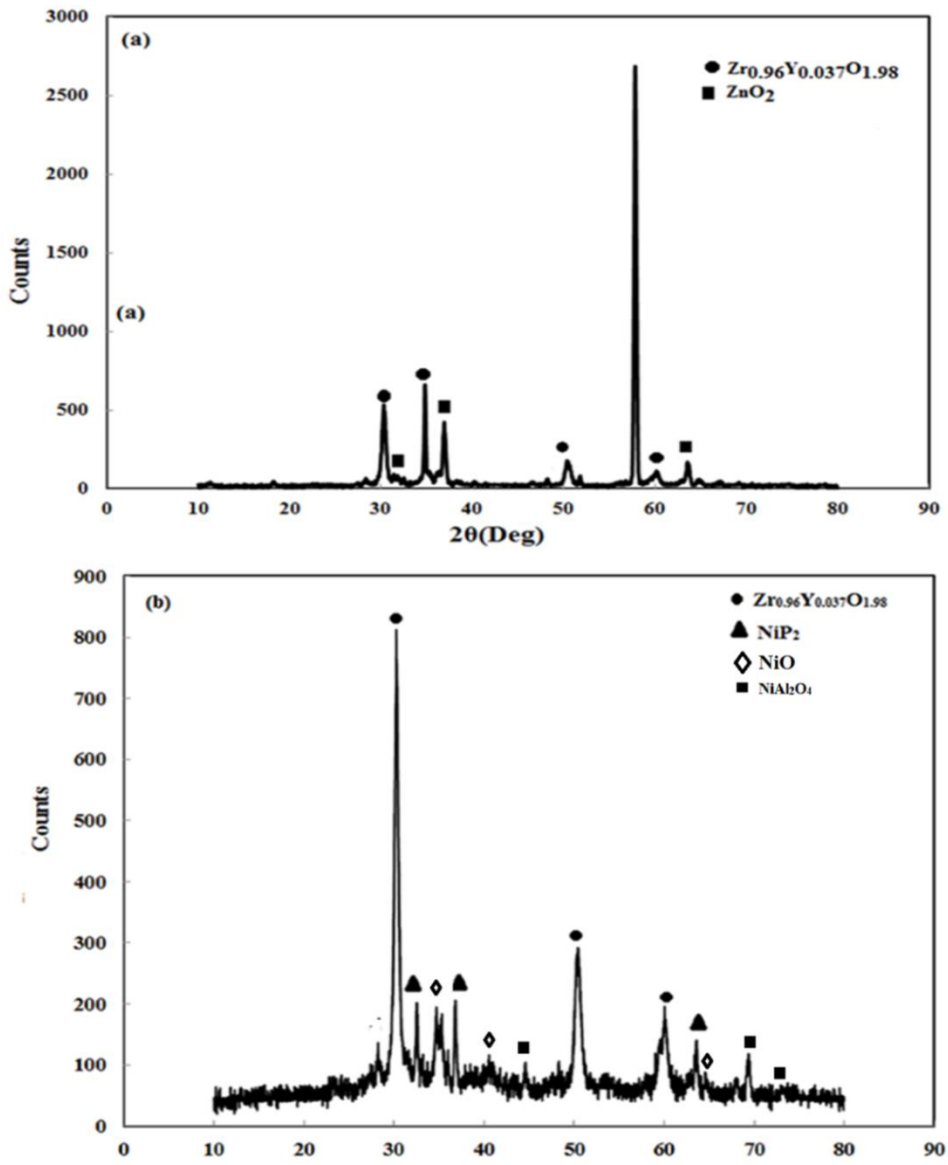

Figure 5: The XRD pattern of YSZ coating on AZ91D, (a) without Ni-P layer and (b) with Ni-P layer.

3.3. EIS analysis of coating

As was mentioned earlier, potentiostatic EIS tests have been carried out at open circuit potential in 3.5% NaCl solution. The Nyquist curves of Figure 6 show the results of these tests. Figure 6(a) illustrates the Nyquist curve for the impedance test performed for AZ91D without coating and Figure 6(b) shows the Nyquist curve related to the test carried out for AZ91D with coatings.

www.SID.ir

The Nyquist diagram of AZ91D reveals a capacitive curve at high and intermediate frequencies. Many authors have related this to the metal dissolution and the oxidation-reduction reactions on the magnesium alloy surface according to equations (9) to (11) [24]. So, its diameter can be associated with charge-transfer resistance and finally associate with the corrosion resistance of the alloy. At low frequencies, a second curve or tail in Nyquist plots reveals an inductive behavior.

$$Mg \rightarrow Mg^{2+} + 2e^{-} \quad (9)$$

$$2H_2O + 2e^{-} \rightarrow H_2 + 2OH^{-} \quad (10)$$

$$Mg + 2H_2O \rightarrow Mg(OH)_2 + H_2 \quad (11)$$

The Nyquist diagram of YNi-AZ sample shows two capacitive curves. The capacitive one at high and medium frequencies can be related to the presence of coatings on the magnesium alloy surface and the low frequencies capacitive arc can be associated with corrosion process on magnesium alloy surface. In addition, an inductive behavior is observed in the Nyquist plot of the magnesium alloy without coating. Numerous examples of such inductive arcs are found in corrosion studies, and various explanations for them have been suggested, mainly involving a potential-dependent adsorption of this part of the impedance plot seems to be rather complicated and is immaterial in studies of electrochemical corrosion, in which the kinetic information is estimated from the capacitive arcs.

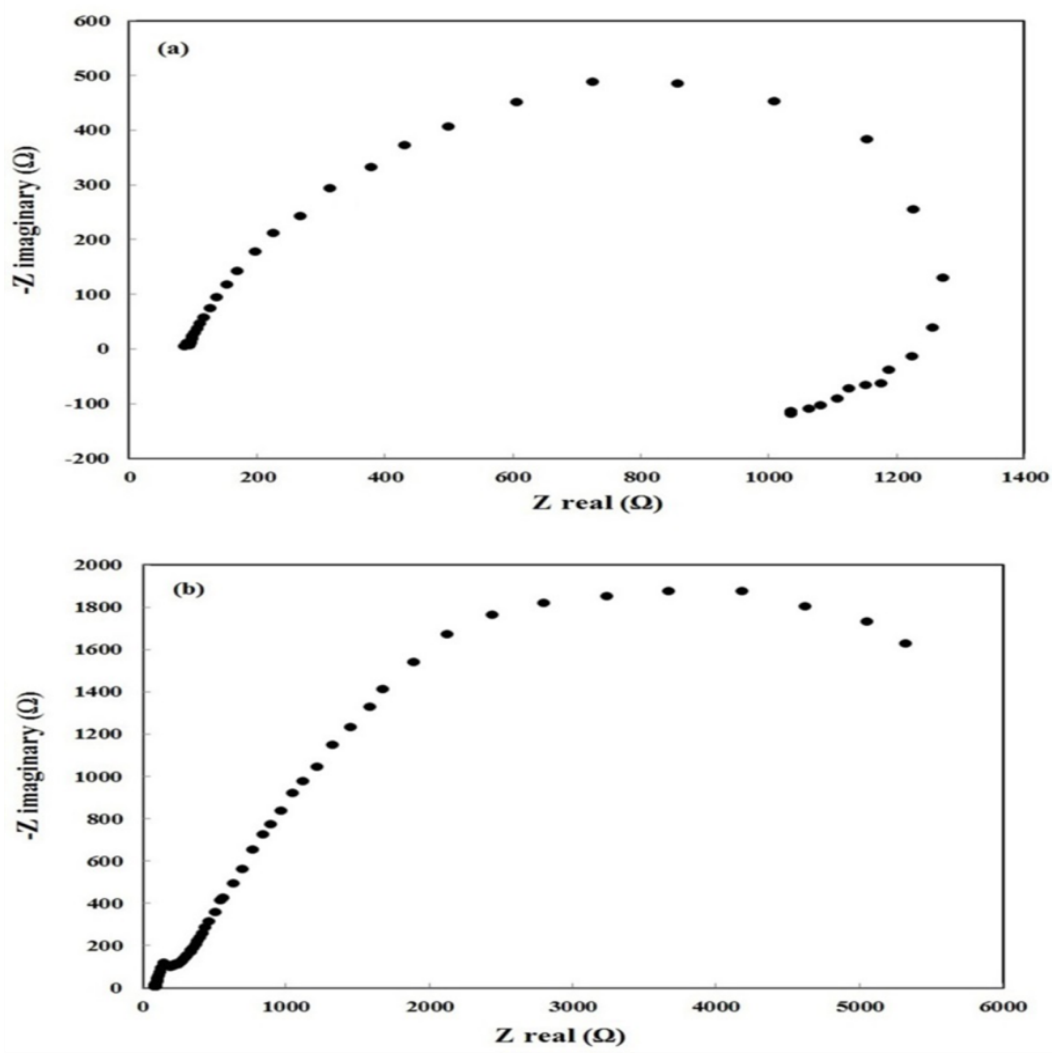

Figure 6: The Nyquist curve of (a) uncoated sample and (b) coated sample.

www.SID.ir

The equivalent circuits used to explain the corrosion behavior of AZ and YNi-AZ samples are shown in Figure 7. The suitable equivalent circuit for analyzing the corrosion behavior of AZ sample is presented in Figure 7 (a). The circuit model for the YNi-AZ is presented in Figure 7(b).

In these circuit models, R_s represents the solution resistance, C_{coat} is the capacitance of the constant phase element (an indicator of the capacity of the coat), and n_1 is the power associated with it. In addition, R_{coat} is the coating resistance, C_{dl} is the double layer constant phase element (an indicator of the double layer capacitance between AZ91D alloy surface and the solution), and n_{dl} is the constant phase element power associated with it, R_t is charge-transfer resistance of the corrosion reaction, L_{adsorp} is the inductance, and R_{adsorp} represents the inductance real resistance. The impedance parameters based on the proposed circuit model were calculated by use of Zview software, in other words using the software's numerical methods, appropriate values are fitted on the measured data and these values are shown in Tables 5 with the sum of weighted squares.

Also, the equation (12) shows the formula for calculating the capacitance of the constant phase element impedance. In this equation, Z_{CPE} is the impedance of the constant phase element, C represents the capacitance, ω stands for the frequency, n is the constant phase element exponent, and it is the imaginary part. It is also worth noting that n varies between 0 and 1 [25].

$$Z_{CPE} = [C(\omega i)^n]^{-1} \quad (12)$$

According to equation (11), by decreasing the capacitance, the capacitive impedance increases. Therefore, in the corrosion process, if the charge-transfer capacitance decreases, it will be expected that the charge- transfer resistance increases. The YSZ and the Ni-P coatings can act as barrier layers which exclude corrosive species from the surface of the magnesium alloy and end to decrease the charge-transfer capacitance of the double layer that is formed between the magnesium alloy and the corrosive solution. So by applying these coatings to AZ91D substrate, the charge transfer resistance of the alloy increases. The results from Table 5 show the effective improvement of the charge transfer resistance of AZ91D with coatings in the chloride solution. On the other hand, the Ni-P layer can act as a cathodic surface on the magnesium alloy surface and can reduce the surface activity of the magnesium alloy.

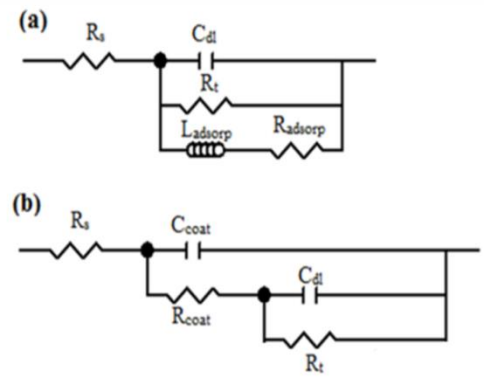

Figure 7: Circuit models proposed for the electrochemical impedance data measured (a) related to uncoated sample and (b) coated sample.

Table 5: Circuit element values calculated by fitting the model presented in Figure 7.

Sample	R_S ($\Omega.cm^2$)	C_{dl} ($\mu F/cm^{-2}$)	n_{dl}	R_t ($\Omega.cm^2$)	C_{coat} ($\mu F/cm^{-2}$)	n_{coat}	R_{coat} ($k\Omega.cm^2$)	L_{adsorp} (kH/cm^2)	R_{adsorp} ($k\Omega.cm^2$)	Sum of weighted squares
AZ	1.87	3.9	0.76	1470.2	---	---	---	4.52	4.9	0.06
YNi-AZ	1.81	4.6	0.81	7032.1	1.01	0.9	322.6	---	---	0.07

Archive of SID
www.SID.ir

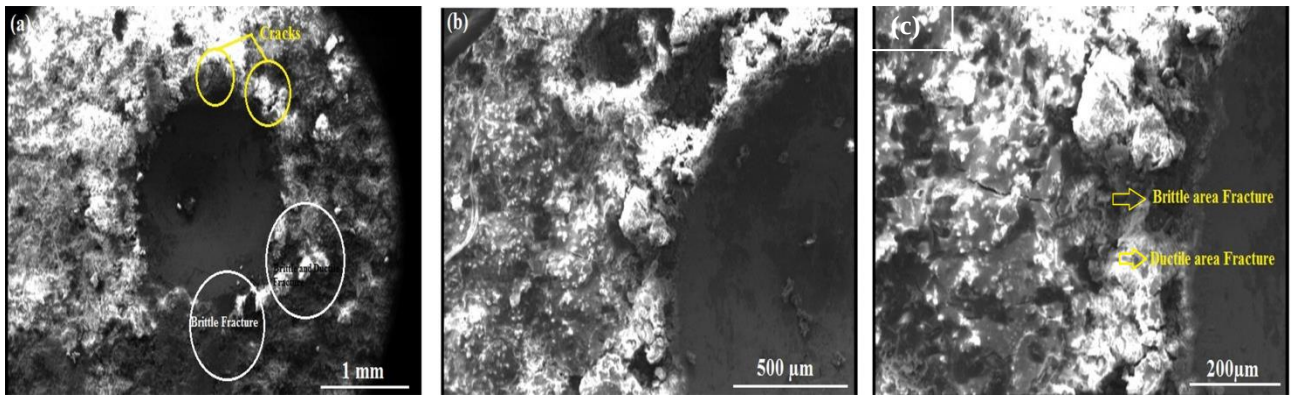

Figure 8: SEM micrograph of coated surface after indentation test, (a) low magnification, (b) and (c) high magnification.

3.4. Indentation analysis coating

The SEM images of the Rockwell indentations are shown in Figure 8. It can be seen that the load of 150 N led to radial plastic deformation of the coating which caused circumferential cracking of the film outside the indentation area. Through-thickness cracks were observed on coating which may be related to the elastic-plastic boundary of the substrates. The indentation marks had a diameter of ~1.6 mm on the coated sample which would cause more deformation at the edge. According to Figure 8, the interfacial bond is adequate, so that, there is some indication of delamination at fracture area of substrate. Also, the radial micro-cracks (identified by white circles in Figure 8) are seen and the fracture of YSZ-Ni-P coating is more brittle, however the ductile areas are seen beside brittle areas as marked by arrows in Figure 8(c). The presence of Ni-P on AZ91D alloy can help to increase the roughness of surface which leads to the increase of effective mechanical interlocking between the YSZ coating and rough substrate. During the EPD process, the presence of Ni-P interlayer results in the formation of hydroxide which can increase the adhesion of YSZ coating to the substrate. Also, the Ni-P layer can bond well to substrate because of the existence of a stronger metal-to-metal bonding during the EN deposition.

4. Conclusion

Deposition of Ni-P layer on AZ91D alloy can hinder the dissolution of AZ91D alloy in acetyl acetone-ethanol solutions and it can help to stabilize suspension of YSZ particles, so that, the agglomeration of YSZ particles on AZ91D alloy with Ni-P layer is less than the agglomeration of YSZ particles on AZ91D alloy without Ni-P layer. Furthermore, after heat treatment at 400°C, the NiP_2 can be produced that can help to increase the corrosion resistance of AZ91D alloy with the YSZ coating in corrosive media. In addition, the Ni-P / YSZ coating improve the corrosion resistance of AZ91D in NaCl solution by increasing the charge-transfer resistance of the surface. The interfacial bond between coating and substrate is adequate that it can be related to the presence of Ni-P interlayer.

5. References

1. M. O. Pekguleryuz, K. Kainer, A. Kaya, Fundamentals of magnesium alloy metallurgy, Woodhead, Philadelphia, 2013, 266-309.
2. J. Gray, B. Luan, Protective coatings on magnesium and its alloys-a critical review, *J. Alloys Compd.*, 336(2002), 88-113.
3. R. G. Hu, S. Zhang, J. F. Bu, C. J. Lin, G. L. Song, Recent progress in corrosion protection of magnesium alloys by organic coatings, *Prog. Org. Coat.*, 73(2012), 129-41.
4. F. Feil, W. Fürbeth, M. Schütze, Purely inorganic coatings based on nanoparticles for

Archive of SID
www.SID.ir

magnesium alloys, *Electrochim Acta.*, 54(2009), 2478-2486.
5. Z. Yao, Y. Xu, Y. Liu, D. Wang, Z. Jiang, F. Wang, Structure and corrosion resistance of ZrO_2 ceramic coatings on AZ91D Mg alloys by plasma electrolytic oxidation, *J. Alloys Compd.*, 509(2011), 8469-74.
6. K. M. Lee, K. R. Shin, S. Namgung, B. Yoo, DH. Shin, Electrochemical response of ZrO^{2-} incorporated oxide layer on AZ91 Mg alloy processed by plasma electrolytic oxidation, *Surf. Coat. Technol.*, 205(2011), 3779-84.
7. L. Stappers, L. Zhang, O. Van der Biest, J. Fransaer, The effect of electrolyte conductivity on electrophoretic deposition, *J. Collo. Inter. Sci.*, 328(2008), 436-46.
8. A. R. Boccaccini, I. Zhitomirsky, Application of electrophoretic and electrolytic deposition techniques in ceramics processing, *Curr. Opin. Solid State Mater. Sci.*, 6(2002), 251-60.
9. I. Zhitomirsky, Cathodic electrodeposition of ceramic and organoceramic materials. Fundamental aspects, *Adv Collo. Inter.*, 97(2002), 279-317.
10. L. Besra, M. Liu, A review on fundamentals and applications of electrophoretic deposition (EPD), *Prog. Mater. Sci.*, 52(2007), 1-61.
11. B. Baufeld, O. Van der Biest, H-J. Rätzer-Scheib, Lowering the sintering temperature for EPD coatings by applying reaction bonding, *J Eur. Ceram. Soc.*, 28(2008), 1793-9.
12. X. Fan, L. Gu, S. Zeng, L. Zhu, C. Wang, Y. Wang, et al, Improving stability of thermal barrier coatings on magnesium alloy with electroless plated Ni-P interlayer, *Surf. Coat. Technol.*, 206(2012), 4471-4480.
13. G. O. Mallory, J. B. Hajdu, Electroless Plating: Fundamentals and Applications, American Electroplaters and Surface Finishers Society, Florida, 1990, 111-138.
14. Z. Wang, P. Xiao, J. Shemilt, Fabrication of composite coatings using a combination of electrochemical methods and reaction bonding process, *J. Eur. Ceram. Soc.*, 20(2000), 1469-73.
15. X. Shu, Y. Wang, J. Peng, P. Yan, B. Yan, X. Fang, et al, Recent Progress in Electroless Ni Coatings for Magnesium Alloys, *Int J Electrochem Sci.*, 10(2015), 1261-73.
16. N. El Mahallawy, A. Bakkar, M. Shoeib, H. Palkowski, V. Neubert, Electroless Ni-P coating of different magnesium alloy, *Surf. Coat. Technol.*, 202(2008), 5151-7.
17. R. Taheri, Evaluation of electroless nickel-phosphorus (EN) coatings, PhD thesis, University of Saskatchewan Saskatoon; Canada, 2002.
18. N. Vidakis, A. Antoniadis, N. Bilalis, The VDI 3198 indentation test evaluation of a reliable qualitative control for layered compounds, *J Mater Process Tech.*, 143-144 (2003), 481-485.
19. Y. Wu, Y. Xiang, W. Hu, C. Zhao, W. Ding, Study on the process of electroless nickel plating on magnesium alloys, *Transactions IMF.*, 83(2005), 91-4.
20. M. Matsuoka, S. Imanishi, T. Hayashi, Physical properties of electroless Ni-P alloy deposits from a pyrophosphate bath, *Plat Surf Finish.*, 76(1989), 54-8.
21. S. Aruna, K. Rajam, A study on the electrophoretic deposition of 8YSZ coating using mixture of acetone and ethanol solvents, *Mater. Chem. Phys.*, 111(2008), 131-6.
22. H. Maleki-Ghaleh, M. Rekabeslami, M. Shakeri, M. Siadati, M. Javidi, S. Talebian, et al. Nano-structured yttria-stabilized zirconia coating by electrophoretic deposition, *Appl. Surf. Sci.*, 280(2013), 666-72.
23. D. Brown, F. Salt, The mechanism of electrophoretic deposition, *J. Appl. Chem.*, 15(1965), 40-8.
24. A. Pardo, M. Merino, A. Coy, F. Viejo, R. Arrabal, S. Feliú, Influence of microstructure and composition on the corrosion behaviour of Mg/Al alloys in chloride media, *Electrochim Acta.*, 53(2008), 7890-902.
25. J. R. Macdonald, E. Barsoukov, Impedance spectroscopy: theory, experiment, and applications, Wiley & Sons, New Jersey , 2005, 87.

How to cite this article:
A. Shahriari, H. Aghajani and M. G. Hosseini, Corrosion Resistance Enhancement of AZ91 Magnesium Alloy Using Ni-P Interlayer and Electrophoretic Deposited 3YSZ Coating, Prog. Color Colorants Coat., 9 (2016) 151-162.

Archive of SID

www.SID.ir

PROGRESS IN COLOR, COLORANTS AND COATINGS

available online @ www.pccc.icrc.ac.ir

Prog. Color Colorants Coat. 9 (2016), 217-222

Ministry of Science, Research and Technology
Institute for Color Science and Technology

پوشش‌دهی الکتروفورتیک 3YSZ بر آلیاژ AZ91 همراه با لایه میانی Ni-P

آیدا شهریاری[۱]، حسین آقاجانی*[۲]، میرقاسم حسینی[۳]

[۱] دانشجوی دکتری، گروه مهندسی مواد، دانشکده مهندسی مکانیک، دانشگاه تبریز، تبریز، ایران، صندوق پستی: ۱۶۴۱-۵۱۶۶۶

[۲] استادیار، گروه مهندسی مواد، دانشکده مهندسی مکانیک، دانشگاه تبریز، تبریز، ایران، صندوق پستی: ۱۶۴۱-۵۱۶۶۶

[۳] استاد، گروه شیمی فیزیک، دانشکده شیمی، دانشگاه تبریز، تبریز، ایران، صندوق پستی: ۱۶۴۱-۵۱۶۶۶

چکیده

زیرکونیای پایدار شده با ۳ درصد مولی اکسید ایتریم (3YSZ) با روش الکتروفورتیک از محلول غیر آبی بر سطح آلیاژ AZ91 اعمال شد. همچنین، لایه میانی Ni-P بین زیرلایه و پوشش 3YSZ با روش الکترولس اعمال شد. در نهایت، زیرلایه همراه با پوشش‌ها در دمای ۴۰۰ درجه سانتی‌گراد در شرایط اتمسفر کنترل شده، عملیات حرارتی شد. آماده سازی پوشش‌ها، میکروساختار و مقاومت به خوردگی آن‌ها بررسی شد. از میکروسکوپ الکترونی روبشی (SEM) به منظور بررسی ریخت شناسی پوشش‌ها استفاده شد. به علاوه، آنالیز فازی سطح با استفاده از پراش اشعه ایکس (XRD) انجام شد. به منظور بررسی مقاومت به خوردگی، روش آنالیز امپدانس الکتروشیمیایی (EIS) در محلول ۳/۵ درصد وزنی کلرید سدیم بکار رفت. همچنین به منظور بررسی پایداری پوشش از آزمون فرورونده راکول سی مطابق استاندار (VDI 3198 norm) استفاده شد. نتایج نشان داد که لایه میانی Ni-P می‌تواند کیفیت پوشش زیرکونیایی را بهبود دهد. همچنین پوشش YSZ-Ni-P، مقاومت به انتقال بار را در سطح آلیاژ AZ91 در محلول کلریدی افزایش می‌دهد.

اطلاعات مقاله

تاریخچه مقاله:

تاریخ دریافت: ۱۵اسفند ۱۳۹۴

تاریخ دریافت آخرین اصلاحات: ۸ اردیبهشت ۱۳۹۵

تاریخ پذیرش: ۲۶ اردیبهشت ۱۳۹۵

در دسترس به صورت الکترونیکی از: ۲۶ اردیبهشت ۱۳۹۵

واژه های کلیدی:

زیرکونیا

پوشش‌دهی الکتروفورتیک

AZ91

لایه میانی Ni-P

*Corresponding author: h_aghajani@tabrizu.ac.ir

Archive of SID

www.SID.ir